Model Development and Model-Based Control Design for High Performance Nonlinear Smart Systems

AFOSR FA9550-04-1-0203

Final Report

for the period
April 1, 2004 - September 30, 2007

Program Manager:

Scott Wells
AFOSR/NM
4015 Wilson Blvd., Room 713
Arlington, VA 22203-8409
scott.wells@afosr.af.mil
703-696-7796

Principal Investigator:

Ralph C. Smith
Center for Research in Scientific Computation
Department of Mathematics
North Carolina State University
Raleigh, NC 27695-8205
rsmith@eos.ncsu.edu
919-515-7552

REPORT DOCUMENTATION PAGE

Form Approved
OMB No. 0704-0188

Public reporting burden for this collection of information is estimated to average 1 hour per response, including the time for reviewing instructions, searching existing data sources, gathering and maintaining the data needed, and completing and reviewing this collection of information. Send comments regarding this burden estimate or any other aspect of this collection of information, including suggestions for reducing this burden to Department of Defense, Washington Headquarters Services, Directorate for Information Operations and Reports (0704-0188), 1215 Jefferson Davis Highway, Suite 1204, Arlington, VA 22202-4302. Respondents should be aware that notwithstanding any other provision of law, no person shall be subject to any penalty for failing to comply with a collection of information if it does not display a currently valid OMB control number. **PLEASE DO NOT RETURN YOUR FORM TO THE ABOVE ADDRESS.**

1. REPORT DATE *(DD-MM-YYYY)*	2. REPORT TYPE	3. DATES COVERED *(From - To)*
20-11-2007	Final Report	01SEP2004-30SEP2007

4. TITLE AND SUBTITLE

Model Development and Model-based control design for high performance nonlinear smart systems

5a. CONTRACT NUMBER
FA9550-04-1-0203

5b. GRANT NUMBER

5c. PROGRAM ELEMENT NUMBER

6. AUTHOR(S)
Ralph Smith

5d. PROJECT NUMBER

5e. TASK NUMBER

5f. WORK UNIT NUMBER

7. PERFORMING ORGANIZATION NAME(S) AND ADDRESS(ES)

North Carolina State

8. PERFORMING ORGANIZATION REPORT NUMBER

9. SPONSORING / MONITORING AGENCY NAME(S) AND ADDRESS(ES)
AFOSR

10. SPONSOR/MONITOR'S ACRONYM(S)

11. SPONSOR/MONITOR'S REPORT NUMBER(S)
AFRL-SR-AR-TR-08-0060

12. DISTRIBUTION / AVAILABILITY STATEMENT
Distribution A: Approved for Public Release

13. SUPPLEMENTARY NOTES

14. ABSTRACT

We have developed a unified energy-based framework for quantifying hysteresis and constitutive nonlinearities inherent to piezoelectric, magnetic, and shape memory compounds which is amenable to inversion and subsequent use as an inverse filter for linear control designs. We have also developed stochastic modeling techniques which quantify the highly complex stiffness properties of ionic polymers in a manner which facilitates design in applications ranging from biological/chemical detection to robotic designfor aerospace structures. The control component has focused on the development of robust linear designs exploiting nonlinear filters and fully nonlinear algorithms which incorporate modeled physics directly into the control design.
Open loop control experiments have been performed and present investigations are focused on closed loop experimental validation of the control theories.

15. SUBJECT TERMS

16. SECURITY CLASSIFICATION OF:			17. LIMITATION OF ABSTRACT	18. NUMBER OF PAGES	19a. NAME OF RESPONSIBLE PERSON
a. REPORT	b. ABSTRACT	c. THIS PAGE			19b. TELEPHONE NUMBER *(include area code)*

Standard Form 298 (Rev. 8-98)
Prescribed by ANSI Std. Z39.18

Objectives

This research program focused on the development of energy-based and stochastic models, numerical approximation techniques, and model-based control designs for piezoelectric, magnetic, ionic polymer, and shape memory alloy actuators and sensors operating in highly nonlinear and hysteretic regimes. The first component of the program focused on the characterization of hysteresis, constitutive nonlinearities, and thermal, stress and frequency-dependencies in a manner that promotes transducer and control design. Secondly, we developed linear and nonlinear control techniques that exploit the physics encapsulated in models to address stringent control objectives (e.g., micron-level tracking, kilohertz to megahertz operating regimes) while operating in highly nonlinear regimes.

Accomplishments

Actuators and sensors comprised of piezoelectric (PZT), magnetic, shape memory alloy (SMA), and ionic polymer components provide unique design and control capabilities for a range of aeronautic and aerospace applications. Piezoelectric compounds are lightweight and provide broadband sensor and actuator capabilities. Furthermore, geometry enhancement of outputs in architectures such as THUNDER (THin layered UNimorph Driver and sEnsoR) transducers provide large strain or displacement capabilities. Due to these attributes, PZT-based devices are presently considered for synthetic jets, shape modification of airfoils, high-speed valve and fuel injector design, and energy harvesting. SMA devices provide the highest work densities of the previously-mentioned materials but are presently limited to frequencies below 100-200 Hz. Within the context of Air Force applications, SMA are being considered for chevron design to reduce jet noise and increase performance, deployment and vibration attenuation in modular antennas, and shape modification of airfoils [22]. Magnetic actuators provide large force capabilities for applications including remote structural deployment as well as high fidelity sensing. Finally, ionic polymers are under development for use in applications ranging from biological/chemical sensing to remote robotics. However, all of these compounds exhibit highly nonlinear dynamics which must be incorporated in models and model-based control designs before their potential can be fully realized in Air Force applications.

Development of a Unified Modeling Framework for Ferroic Compounds

A hallmark of this program was the development of a unified characterization framework for ferroelectric (e.g., PZT), ferromagnetic, and ferroelastic (e.g., SMA) materials — which are collectively designated as ferroic compounds. As detailed in [22, 29], the framework is constructed in two steps. In the first, Helmholtz and Gibbs energy relations are constructed at the mesoscopic, or lattice, scale to quantify the local average polarization, magnetization, or strain. In the second step, stochastic homogenization techniques are invoked to construct macroscopic models that incorporate the effects of material nonhomogeneities, polycrystallinity, and nonuniform effective fields. The resulting models are sufficiently accurate for material characterization and sufficiently efficient to facilitate model-based control design.

We summarize here primary steps in the framework and note that details regarding the framework can be found in [22–24, 27, 29]. Extensions the theory to incorporate stress and temperature-dependence are provided in [1, 2, 4, 6, 10, 16, 21, 26, 28].

Let P, M and ε respectively denote polarization, magnetization and strains and let E, H and σ denote an applied electric field, magnetic field, and stress. One can consolidate notation by letting $e = P, M, \varepsilon$ denote an order parameter and let $\varphi = E, H, \sigma$ denote conjugate fields. Additionally, we let q designate electromechanical or magnetomechanical coupling coefficients.

In the first step of the development, we consider the Gibbs energy relations

$$\begin{aligned} G(E,P,T) &= \psi(P,T) - EP - \sigma\varepsilon \qquad \text{Ferroelectric} \\ G(H,M,T) &= \psi(M,T) - HM - \sigma\varepsilon \qquad \text{Ferromagnetic} \\ G(\sigma,\varepsilon,T) &= \psi_\varepsilon(\varepsilon,T) - \sigma\varepsilon \qquad \text{Ferroelastic} \end{aligned} \tag{1}$$

where T is temperature in degrees Kelvin. For ferroelectric ($e = P$) and ferromagnetic ($e = M$) materials, the the Helmholtz energy relations have the form

$$\psi(e,T) = \psi_e(e,T) + \frac{1}{2}Y^e\varepsilon^2 - q\varepsilon(e - e_R)^2 \tag{2}$$

where the piecewise quadratic component ψ_e incorporates the bistable behavior associated with equilibrium dipole or moment configurations as depicted in Figure 1(a). The second and third terms on the right side of (2) incorporate the elastic and electromechanical or magnetomechanical coupling energy. For ferroelastic materials, ψ_ε characterizes the tristable martensite-austenite phase behavior shown in Figure 1(b).

For regimes in which thermal activation is negligible, piecewise linear kernel relations of the form

$$\overline{P} = \frac{E}{\eta - 2q\varepsilon} + \frac{2q\varepsilon - \Delta\eta}{\eta - 2q\varepsilon}P_R, \tag{3}$$

where $\Delta = \pm 1$, are obtained through enforcement of the equilibrium conditions $\frac{\partial G}{\partial P} = 0$. The relations for $\overline{M}$ and $\overline{\varepsilon}$ are similar.

To incorporate thermal activation, which is manifested at the macroscopic level as creep, relaxation, reptation, or accommodation, it is necessary to balance the Gibbs energy with the relative thermal energy kT/V via the Boltzmann relation

$$\mu(G) = Ce^{-GV/kT}. \tag{4}$$

Here k, V and C respectively denote Boltzmann's constant, a reference volume, and an integration constant. This yields kernel or hysteron relations of the form

$$\begin{aligned} \overline{e} &= x_+ \langle e_+ \rangle + x_- \langle e_- \rangle \\ \overline{\varepsilon} &= x_+ \langle \varepsilon_+ \rangle + x_- \langle \varepsilon_- \rangle + x_A \langle \varepsilon_A \rangle \end{aligned} \tag{5}$$

where x_+, x_-, x_A are moment, dipole or phase fractions and the bracketed quantities denote average polarizations, magnetizations, or strains associated with specified dipole, moment or phase configurations.

In the second step of the development, the effects of polycrystallinity, material nonhomogeneities, and variable conjugate fields are incorporated by assuming that certain material properties (e.g.,

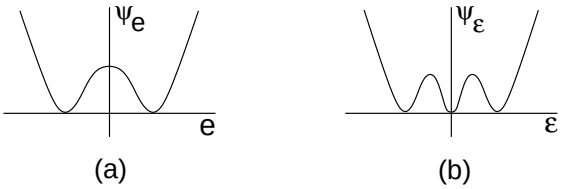

Figure 1: Helmholtz energy for (a) ferroelectric or ferromagnetic materials, and (b) ferroelastic materials.

coercive fields E_c, H_c, interaction fields E_I, H_I, σ_I and relative stresses σ_R) are manifestations of underlying distributions rather than constants. We denote corresponding densities by ν_1 and ν_2. Enforcement of the equilibrium conditions $\frac{\partial G}{\partial \varepsilon} = 0$ and incorporation of Kelvin–Voigt damping subsequently yields the constitutive relations

$$\begin{cases} [P(E,T)](t) = \displaystyle\int_0^\infty \int_{-\infty}^\infty [\overline{P}(E+E_I,T;E_c)\nu_1(E_c)\nu_2(E_I)dE_I dE_c \\ \sigma = Y\varepsilon + c\dot{\varepsilon} - q(P-P_R)^2, \end{cases} \tag{6}$$

$$\begin{cases} [M(H,T)](t) = \displaystyle\int_0^\infty \int_{-\infty}^\infty [\overline{M}(H+H_I,T;H_c)\nu_1(H_c)\nu_2(H_I)dH_I dH_c \\ \sigma = Y\varepsilon + c\dot{\varepsilon} - q(M-M_R)^2, \end{cases} \tag{7}$$

$$\begin{cases} [\varepsilon(\sigma,T)](t) = \displaystyle\int_0^\infty \int_{-\infty}^\infty [\overline{\varepsilon}(\sigma+\sigma_I,T;\sigma_R)\nu_1(\sigma_R)\nu_2(\sigma_I)d\sigma_R d\sigma_R \end{cases} \tag{8}$$

for ferroelectric, ferromagnetic and ferroelastic materials.

Temperature changes due to convection, conduction, dipole/moment switching or phase changes, and Joule heating can be quantified by the general relation

$$\bar{c}\mathcal{M}\dot{T}(t) = -\Omega[h_c + \lambda/\ell][T(t) - T_E(t)] + J(t) - \sum_\alpha h_\alpha \dot{x}_\alpha. \tag{9}$$

Here $\bar{c}, \mathcal{M}, h_c, \Omega, \lambda, \ell$ and $T_E(t)$ respectively denote the specific heat for the actuator material, the mass of the actuator, a convection coefficient, the surface area of the material, the thermal conductivity of the surrounding medium, the interval over which conduction occurs, and the time varying temperature of the adjacent environment. The components $-h_c\Omega[T(t)-T_E(t)]$ and $-\lambda\Omega[T(t)-T_E(t)]/\ell$ respectively quantify the effects of convection and conduction, and $J(t)$ characterizes Joule heating mechanisms. The final component quantifies heat transduction due to dipole/moment switching or phase transitions so that h_α represents specific enthalpies.

In combination, relations (6) – (9) characterize the 1-D constitutive behavior of PZT, magnetic materials, and SMA, and provide a framework for constructing distributed actuator and sensor models. The performance of this modeling framework is illustrated for nickel, PZT, and thin film SMA in Figure 2 through a comparison and prediction of experimental data. This illustrates both the accuracy of the methodology for a variety of regimes including biased minor loops which exhibit nonclosure due to thermal relaxation or creep mechanisms — e.g., the nickel data and fit in Figure 2(a) and (b).

Structural Models

Electromechanical and magnetomechanical constitutive relations of the form (6) and (7) provide the basis for constructing structural models for systems employing ferroelectric or magnetic sensors. To illustrate, consider a piezoelectric (ferroelectric) rod having cross-sectional area A, length ℓ, density ρ, Young's modulus Y, Kelvin-Voigt damping coefficient c, a fixed end at $x = 0$ and a free end at $x = \ell$. As detailed in Chapter 7 of [22], force balancing yields the relation

$$\rho A \frac{\partial^2 u}{\partial t^2} = A\frac{\partial \sigma}{\partial x} \tag{10}$$

where σ is specified in (6) and u denotes the longitudinal displacement. Use of the linear strain-displacement relation $\varepsilon = \frac{\partial u}{\partial x}$ and integration by parts yields the weak model formulation

$$\int_0^\ell \rho A \frac{\partial^2 u}{\partial x^2}\phi dx + \int_0^\ell YA\frac{\partial u}{\partial x}\frac{d\phi}{dx}dx + \int_0^\ell cA\frac{\partial^2 u}{\partial x \partial t}\frac{d\phi}{dx}dx = Aq(P-P_R)^2\int_0^\ell \frac{d\phi}{dx}dx \tag{11}$$

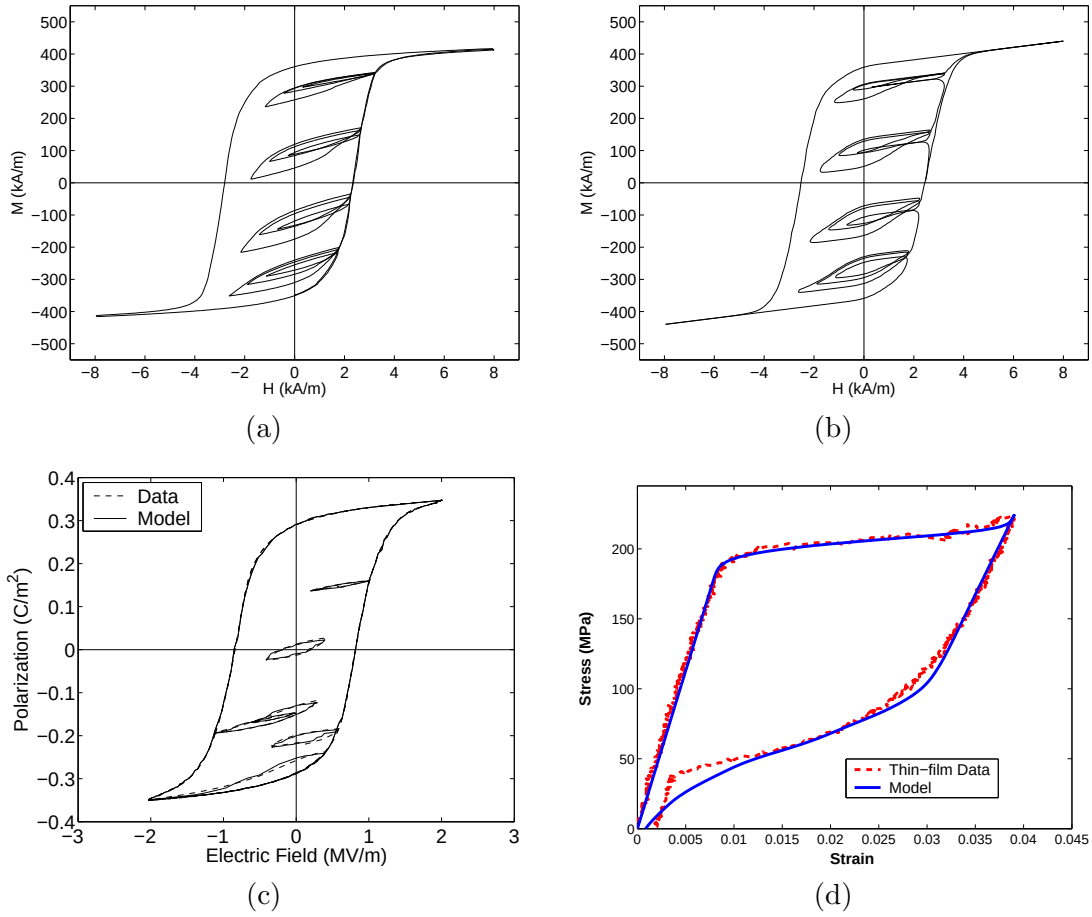

Figure 2: (a) Nickel 200 H-M data, and (b) H-M model fit for multiple biased minor loops from [24]. (c) Model comparison to quasistatic PZT5H data from [27], and (d) model fit to thin film SMA data from [10].

for all test functions $\phi \in H_0^1(0,\ell)$ and P given by (6). This provides a framework appropriate for approximation and subsequent model-based control design. Similar analysis is provided for beams, plates and shells in [22].

Stochastic Models for Ionic Polymers

Ionic polymers exhibit a highly complex structure comprised of a hydrophobic backbone and hydrophilic side chains which presently precludes energy analysis in a manner that permits real-time implementation. During this program, we have developed stochastic models at the molecular level which can be employed in low-order macroscopic models to predict effective material properties such as stiffness [11,30]. By employing analytic density estimation techniques, the macroscopic models are sufficiently efficient to permit both actuator/sensor characterization and to consider the significantly more difficult inverse problem of material design to achieve specified control criteria. This provides an initial step toward the development of a paradigm to custom design materials to optimally achieve control criteria for Air Force Applications.

Parameter Estimation

A crucial step for model construction or updating is the development of highly robust parameter estimation techniques to identify the densities, and other model parameters, based on attributes of

the data with little input required from users. To achieve this, we have developed theory and Graphical User Interface (GUI)-based packages that provide initial parameter estimates based solely on measured properties of the data [25]. Representative fits to frequency-dependent data are illustrated in Figure 3. We note that these fits required approximately 4 minutes of CPU time on a personal computer and hence the algorithms are sufficiently efficient to permit rapid model construction.

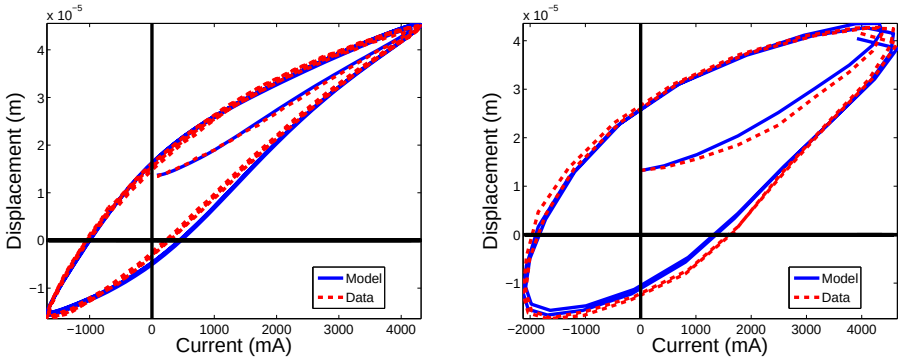

Figure 3: Model fit to magnetic displacement data collected at (a) 100 Hz and (b) 500 Hz.

High Speed FPGA Implementation

High speed, high accuracy Air Force applications dictate that model-based control techniques be implemented at kilohertz to megahertz rates. For the homogenized energy model, this means that quadratures associated with the formulations (6) – (8) and construction of the hysterons (5) must be performed in microseconds. To achieve these rates, we initiated investigations regarding the use of field programmable gate arrays (FPGA). These user-configurable hardware chips combine tens to hundreds of thousands of look-up tables, flip-flops, and switches that can be programmed by a user to achieve a custom design. These devices are naturally parallelizable which proves highly advantageous when constructing hysterons and numerically approximating the integrals.

As detailed in [3, 5], the use of FPGA yields speedups of approximately 100-fold for the thermal relaxation model as compared with optimized C implementations. Depending on the number of quadrature points, this yields implementation rates in the kilohertz range for inverse models which is sufficiently fast for real-time control implementation of high speed Air Force applications.

Model-Based Control Design: Nonlinear Inverse Compensators

The goal of the control component of the investigation was to develop theory and algorithms that permit real-time tracking and vibration attenuation using smart material actuators operating in highly nonlinear and hysteretic regimes. For the applications under consideration, this can result in micron-level (or smaller) tolerances and quasistatic up to kilohertz operating frequencies.

As depicted in Figure 4, there are essentially two control strategies for hysteretic systems using nonlinear models. The first is to use the characterization framework to construct an approximate nonlinear inverse that linearizes the actuator response in the manner depicted in Figure 4(a). Linear control algorithms are then used to achieve control objectives. The second strategy is to construct nonlinear control designs which yield input signals that directly incorporate actuator nonlinearities as depicted in Figure 4(b). The latter strategy is advantageous when tracking trajectories are known *a priori* whereas the inverse compensators will be required when attenuating unmodeled or stochastic uncertainties.

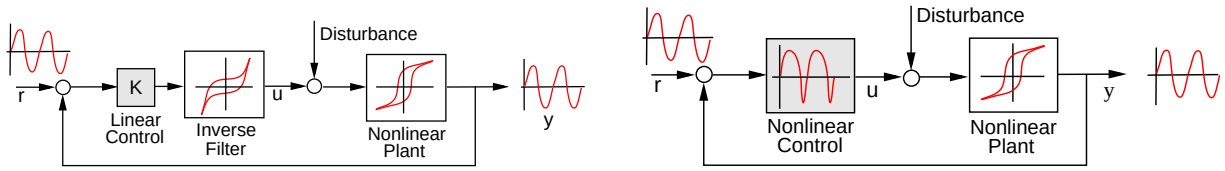

Figure 4: (a) Linear control design employing a nonlinear, model-based inverse compensator and (b) nonlinear model-based control design.

During this program, we developed highly efficient inverse model formulations, based on the homogenized energy framework, that provide a significant step toward real-time implementation capabilities. As detailed in [4], these inverse algorithms employ either lookup tables or rational function approximations in the forward models in combination with fixed-point algorithms to construct highly efficient inverse representations. The accuracy of these inverse models is illustrated in Figure 5. Present C implementations of these inverse models run at 500 to 1000 Hz whereas FPGA implementations are projected to be approximately 2 orders of magnitude faster.

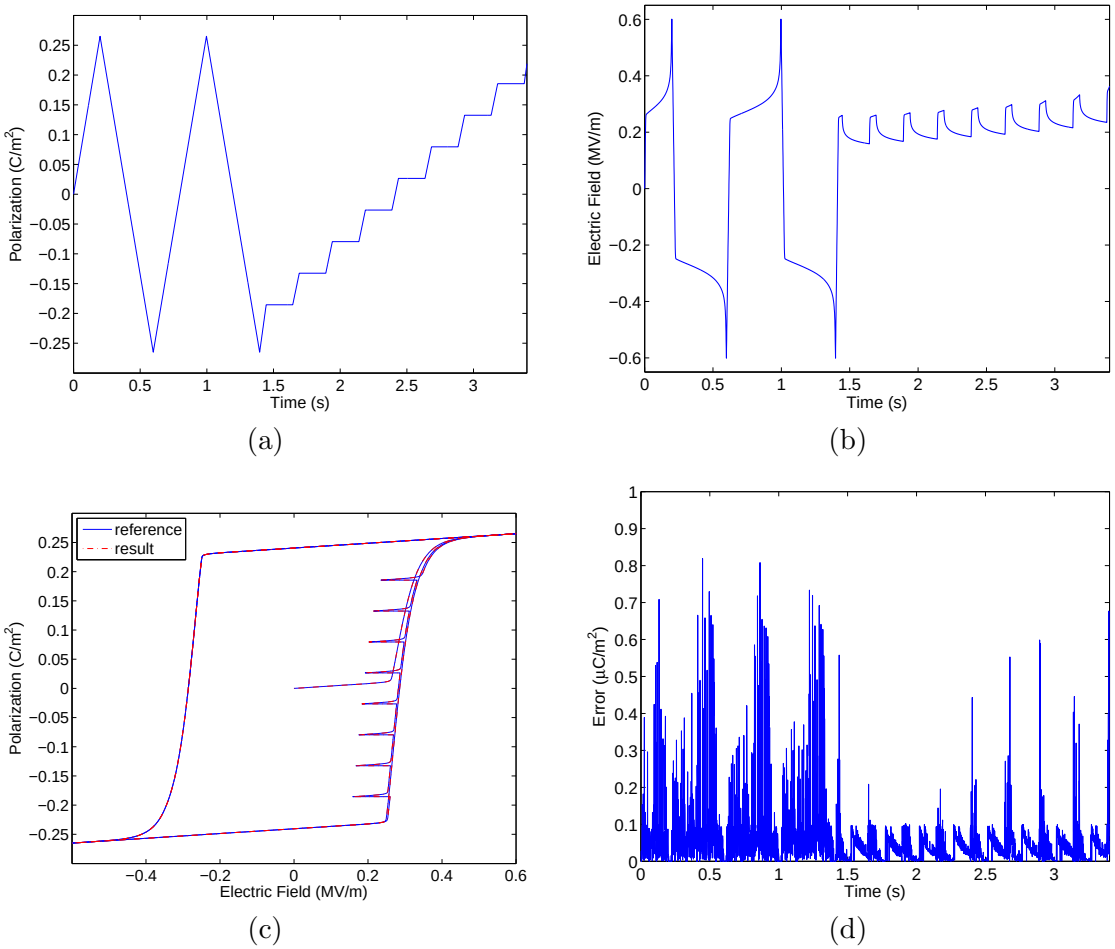

Figure 5: (a) Reference polarization $\widehat{P}$, and (b) electric field E given by the inverse model with parameters estimated for PLZT. (c) Comparison of the polarization P given by (6) with input E and the reference polarization $\widehat{P}$, and (d) the absolute error $|\widehat{P} - P|$.

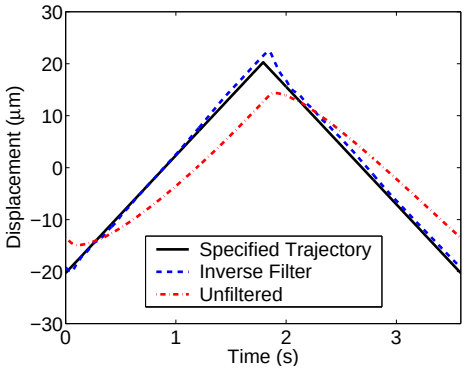

Figure 6: Tracking performance in open loop experiments utilizing a model-based inverse and in the absence of a filter.

We have also investigated numerical algorithms and experimental implementation of open loop designs employing inverse filters based on the homogenized energy framework. These results are reported in [8, 9, 12] with representative experimental tracking results for filtered and unfiltered designs shown in Figure 6.

Model-Based Control Design: Nonlinear Optimal Control

The second main thrust of the control component of the program has focused on the formulation, numerical implementation, and experimental implementation of nonlinear perturbation control designs for systems employing PZT and magnetic actuators operating in hysteretic regimes. As detailed in [13–15, 17–20], these designs are developed in two steps: (i) construction of an optimal nonlinear open loop control signal, and (ii) construction of a perturbation feedback component obtained through linearization about the optimality system.

To illustrate, let r denote a reference signal to be tracked, $y(t) = Cx(t)$ denote observations and let $e(t) = Cx(t) - r(t)$ designate the error. The augmented penalty functional is taken to be

$$\overline{J} = \frac{1}{2}[Cx(t_f) - r(t_f)]^T P[Cx(t_f) - r(t_f)] + \int_{t_0}^{t_f} \left[\mathcal{H} - \lambda^T(t)\dot{x}(t)\right] \, dt \tag{12}$$

where λ denotes the adjoint variable, the Hamiltonian is

$$\mathcal{H} = \frac{1}{2}[e(t)^T Q e(t) + u^T(t) R u(t)] + \lambda^T \left[Ax(t) + [B(u)](t)\right], \tag{13}$$

and Q, R respectively penalize large errors and control inputs.

Enforcement of necessary conditions to minimize (12) yields the control input relation

$$u^*(t) = -R^{-1} \left(\frac{\partial B(u)}{\partial u}\right)^T \lambda(t) \tag{14}$$

along with the two-point boundary value problem

$$\dot{z}(t) = F(t, z) \tag{15}$$

where $z = [x, \lambda]^T$ and

$$F(t,z) = \begin{bmatrix} Ax(t) + [B(u)](t) \\ -A^T\lambda(t) - C^T Q C x(t) + C^T Q r(t) \end{bmatrix}. \tag{16}$$

To approximate the solution to (15), we employ a finite difference discretization defined on the grid $t_j = j\Delta t$, where $\Delta t = \frac{t_f}{N}$ and $j = 0, \cdots, N$. Letting $z_j \approx z(t_j)$, this yields the discrete system

$$\begin{aligned} &\frac{1}{\Delta t}\left[z_{j+1} - z_j\right] = \frac{1}{2}\left[F(t_j, z_j) + F(t_{j+1}, z_{j+1})\right] \\ &E_0 z_0 = [x_0, 0]^T \\ &E_f z_N = [0, -C^T P r(t_f)]^T. \end{aligned} \tag{17}$$

The solution of (17) can be expressed as the problem of finding $z_h = [z_0, \cdots, z_N]$ which solves

$$\mathcal{F}(z_h) = 0. \tag{18}$$

A quasi-Newton iteration of the form

$$z_h^{k+1} = z_h^k + \xi_h^k, \tag{19}$$

where ξ_h^k solves

$$\mathcal{F}'(z_h^k)\xi_h^k = -\mathcal{F}(z_h^k), \tag{20}$$

is then used to approximate the solution to (18). The Jacobian has the form

$$\mathcal{F}'(z_h) = \begin{bmatrix} S_0 & R_0 & & & & \\ & S_1 & R_1 & & & \\ & & \ddots & \ddots & & \\ & & & & S_{N-1} & R_{N-1} \\ E_0 & & & & & E_f \end{bmatrix} \tag{21}$$

where

$$S_i = -\frac{1}{\Delta t}\begin{bmatrix} I & 0 \\ 0 & I \end{bmatrix} - \frac{1}{2}\begin{bmatrix} A & \frac{\partial}{\partial \lambda} B[u_i^*] \\ -C^T Q C & -A^T \end{bmatrix}. \tag{22}$$

The representation for R_i is similar.

It is shown in [18, 19] that an analytic LU decomposition can be determined for $\mathcal{F}(z_h^k)$. This significantly reduces memory requirements and is fundamental for efficient solution.

The relation (14) provides an open loop control signal that is optimal for given Q, R in the absence of model or measurement error. To provide robustness with regard to such uncertainties, we consider perturbation feedback. Linearization about the optimality system yields

$$\begin{aligned} \delta\dot{x}(t) &= A\delta x(t) + B\delta u(t) \\ \delta y(t) &= C\delta x(t) \end{aligned} \tag{23}$$

where $\delta u, \delta x$ and δy are first-order variations about u^*, x^* and y^*.

To facilitate experimental implementation, we use classical PI control to compute δu; that is, we take

$$\delta u(t) = -K_P e(t) - K_I \int_0^t e(s) ds. \tag{24}$$

The final control input is then

$$u(t) = u^*(t) + \delta u(t). \tag{25}$$

The performance of this perturbation control in tracking experiments, conducted at 1 kHz, is illustrated in Figure 7. The results in Figure 7(a) illustrate that an optimized PI design, in the absence

of the nonlinear open loop signal, exhibits significant errors in both the phase and amplitude due to the frequency-dependent hysteresis shown in Figure 7(b). The perturbation control accommodates this nonlinear behavior and achieves accurate tracking. This is an approximately 30-fold improvement in operating frequency over previous control techniques based on Preisach models.

A crucial aspect of this approach is the fact that the optimal open loop control signals are constructed offline and hence implementation speeds are dictated by the efficiency of the perturbation feedback algorithm. The experimental results at 1 kHz demonstrate the potential of the technique for applications that require high-speed tracking or broadband vibration attenuation using actuators that are operating in highly hysteretic and nonlinear regimes.

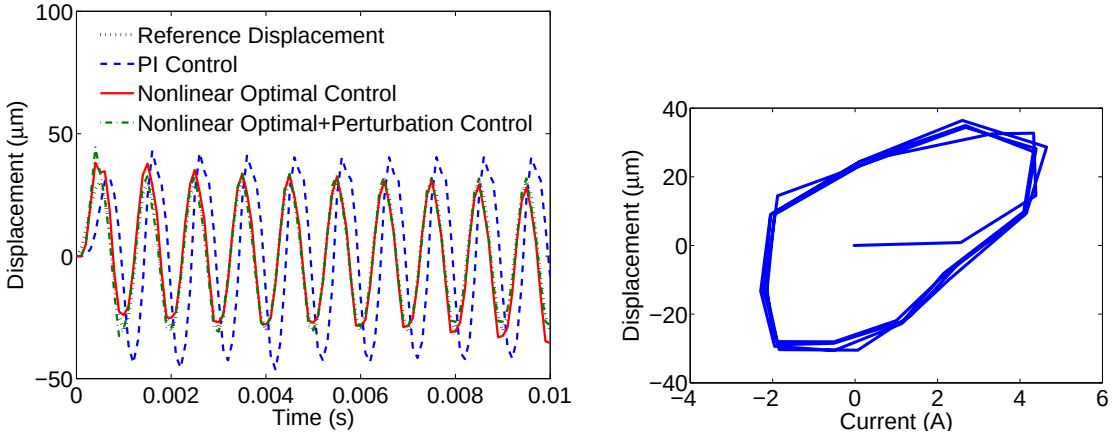

(a) (b)

Figure 7: (a) Reference trajectory and experimental tracking performance obtained with PI control, optimal open loop control and perturbation control at 1000 Hz. (b) Hysteretic and nonlinear input-output behavior of the magnetic actuator.

Personnel Supported

Brian Ball	Graduate Student, NCSU, Raleigh, NC
Jon Ernstberger	Graduate Student, NCSU, Raleigh, NC
Xiang Fan	Graduate Student, NCSU, Raleigh, NC
Emily Lada	Postdoc, NCSU, Raleigh, NC
William Oates	Postdoc, NCSU, Raleigh, NC
Ralph Smith	Professor, NCSU, Raleigh, NC
Heather Wilson	Graduate Student, NCSU, Raleigh, NC

Interactions/Transitions

Conference, Colloquia and Workshop Presentations

- Department of Mathematics, Clemson University, April 18, 2004
- World Congress of Nonlinear Analysts, Orlando, FL, July 8, 2004
- SIAM Annual Meeting, Portland, OR, July 14, 2004
- 43rd IEEE Conference on Decision and Control, Paradise Island, The Bahamas, December 16, 2004.

- Department of Math. Sciences, Montana State University, February 10, 2005.
- SPIE's 12th Annual Symposium on Smart Structures and Materials, San Diego, CA, March 9, 2004.
- 2005 U.S. Navy Workshop on Acoustic Transduction Materials and Devices, State College, PA, May 12, 2005.
- SIAM Annual Meeting, New Orleans, LA, July 13, 2005.
- ICAM Workshop on Mathematics as an Enabling Science, Blacksburg, VA, October 1, 2005.
- ASME International Mechanical Engineering Congress and Exposition, Orlando, FL, November 9, 2005.
- SPIE's 13th Annual Symposium on Smart Structures and Materials, San Diego, CA, February 28, 2006.
- SIAM-SEAS 30th Annual Meeting, Auburn University, Auburn, AL, March 31, 2006 (Plenary Presentation).
- CSRI Workshop on Numerical PDEs in the 21st Century, Albuquerque, NM, April 21, 2006.
- Fourth World Conference on Structural Control and Monitoring, San Diego, CA, July 12, 2006 (Keynote Presentation).
- ICAT 47th International Smart Actuator Symposium, Penn State University, State College, PA, October 4, 2006.
- Department of Mathematical Sciences, Montana State University, Bozeman, MT, November 30, 2006.
- 45th IEEE Conference on Decision and Control, San Diego, CA, December 14, 2006.
- Department of Mechanical Engineering, Florida State University, Tallahassee, FL, February 1, 2007.
- Idaho National Laboratory, Idaho Falls, ID, March 15, 2007.
- Department of Mathematics, University of Waterloo, Waterloo, Ontario, April 26, 2007.
- Oak Ridge National Laboratory, Oak Ridge, TN, May 1, 2007.
- 2007 U.S. Navy Workshop on Acoustic Transduction Materials and Devices, Penn State University, State College, PA, May 15, 2007.
- SIAM Conference on Control and Its Applications, San Francisco, CA, June 29, 2007.

Transitions

1. *Magnetostrictive Actuators – Etrema:* The nonlinear magnetic constitutive models and perturbation control techniques reported here are being extended, in collaboration with scientists at Etrema Products, to optimize the performance of Active Machining Systems (AMS) used to mill products such as piston heads. The goal is to significantly increase milling speeds (e.g., up

to 20,000 cycles per second) while maintaining micron-level accuracy. The Etrema and AFOSR investigations are mutually complementary and each provides substantial technology transfer to the other. Point of Contact: Rick Zrostlik, Etrema Products Inc., Ames, IA, 515-296-8030.

2. *SMA Chevrons and Torque Tubes – Boeing:* The 1-D SMA models developed through the AFOSR program are being extended in collaboration with Boeing scientists to 2-D and 3-D geometries inherent to chevrons used to reduce jet noise and decrease drag with potential application to improved inlet channel design. Similar models are being considered by Boeing as optimization tools for the design of SMA torque tubes to change the camber of rotorcraft blades. In both cases, models and control designs will be validated using data from Boeing experiments and flight tests. Point of contact: James Mabe, Boeing Phantom Works, Seattle, WA, 206-655-0091.

3. *PZT Unimorphs – Boeing:* Nonlinear structural models developed through AFOSR support are being considered at Boeing for characterizing the hysteretic and nonlinear behavior of PZT-based unimorphs under investigation for flow control and improved flight capabilities. The second phase of the investigation will focus on model-based control design and implementation of the unimorphs. This can potentially impact a broad range of flow control problems of interest to the Air Force and Boeing. Point of contact: James Mabe, Boeing Phantom Works, Seattle, WA, 206-655-0091.

4. *SMA Thin Films and MEMs – Sandia:* Shape memory alloy models developed through AFOSR support are being investigated at Sandia National Laboratories for characterization and control design in applications employing shape memory films and MEMs. The potential benefit to the Air Force mission is significant since SMA films and MEMs retain the high strain properties of bulk SMA but have the potential for operating at significantly higher frequencies. Point of contact: James Redmond, Sandia National Laboratories, Albuquerque, NM, 505-844-3136.

5. *Nanopositioning – Asylum Research:* The models quantifying constitutive nonlinearities, hysteresis, thermal effects, and frequency effects in piezoceramic materials will be employed in conjunction with model-based control laws to improve the resolution and efficiency of nanopositioners including high speed scanning for atomic force microscopy. Point of contact: Jason Cleveland, Asylum Research, Santa Barbara, CA, 805-692-2800.

6. *SMA Polymers – AFRL:* We are initiating investigations to extend the shape memory alloy models developed through AFOSR support to shape memory resins and polymers presently being considered by AFRL researchers for deployment of gossamer structures. The SMA polymers provide the work density requirements necessary to deploy aerospace structures such as radar antennas and large optical mirrors but exhibit viscoelastic and thermodynamic attributes that are not accommodated by present models or control techniques. Point of contact: Thomas Murphey, Kirtland AFB, Albuquerque, NM, 505-846-9969.

Publications

Refereed publications resulting from work supported by this grant are listed as references.

References

[1] B.L. Ball, R.C. Smith, S-J. Kim and S. Seelecke, "A stress-dependent hysteresis model for ferroelectric materials," *Journal of Intelligent Material Systems and Structures*, 18(1), pp.69–88, 2007.

[2] T.R. Braun and R.C. Smith, "Efficient implementation algorithms for homogenized energy models," *Continuum Mechanics and Thermodynamics*, 18(3-4), pp. 137–155, 2006.

[3] T.R. Braun and R.C. Smith, "FPGA-Based Model Implementation for Real-Time Control of Smart Material Systems Operating in Hysteretic Regimes," Cansmart 2007, International Workshop on Smart Materials and Structures, Montreal, Quebec, CN, October 10-11, 2007.

[4] T.R. Braun and R.C. Smith, "High speed model implementation and inversion techniques for ferroelectric and ferromagnetic transducers," *Journal of Intelligent Material Systems and Structures*, to appear.

[5] T.R. Braun and R.C. Smith, "High speed FPGA model implementation for ferroelectric and ferromagnetic transducers," *Journal of Computational Physics*, submitted.

[6] T.R. Braun, R.C. Smith and M.J. Dapino, "Experimental validation of a homogenized energy model for magnetic after-effects," *Applied Physics Letters*, 88, pp. 122511–122513, 2006.

[7] M.A. Demetriou, K. Ito and R.C. Smith, "On-line monitoring and accommodation of nonlinear actuator faults in positive real infinite dimensional systems," Proc 43rd IEEE Conf. Dec. and Control, Paradise Island, The Bahamas, pp. 2871-2875, 2004.

[8] A.G. Hatch, R.C. Smith and T. De, "Experimental implementation of a model-based inverse filter to attenuate hysteresis in an atomic force microscope," Proc 43rd IEEE Conf. Dec. and Control, Paradise Island, The Bahamas, pp. 3062-3067, 2004.

[9] A.G. Hatch, R.C. Smith, T. De and M.V. Salapaka, "Construction and experimental implementation of a model-based inverse filter to attenuate hysteresis in ferroelectric transducers," *IEEE Transactions on Control Systems Technology*, 14(6), pp. 1058–1069, 2006.

[10] J.E. Massad and R.C. Smith, "A homogenized free energy model for hysteresis in thin-film shape memory alloys," *Thin Solid Films*, 489(1-2), pp. 266-290, 2005.

[11] J.L. Matthews, E.K. Lada, L.M. Weiland, R.C. Smith and D.J. Leo, "Monte Carlo simulation of a solvated ionic polymer with cluster morphology," *Smart Materials and Structures*, 15, pp. 187–199, 2006.

[12] J.M. Nealis and R.C. Smith, "Model-based robust control design for magnetostrictive transducers operating in hysteretic and nonlinear regimes," *IEEE Transactions on Control Systems Technology*, 15(1), 2007.

[13] W.S. Oates, P. Evans, R.C. Smith and M.J. Dapino, "Experimental implementation of a nonlinear control method for magnetostrictive transducers," Proceedings of the 2007 American Control Conference, New York, NY, to appear.

[14] W.S. Oates, P.G. Evans, R.C. Smith and M.J. Dapino, "Experimental implementation of a hybrid nonlinear control design for magnetostrictive actuators," *Journal of Dynamic Systems, Measurement, and Control*, submitted.

[15] W.S. Oates and R.C. Smith, "Nonlinear open loop optimal tracking using magnetostrictive transducers," Proceedings of the 2005 ASME International Mechanical Engineering Congress and Exposition, Orlando, FL, IMECE2005-79898.

[16] W.S. Oates and R.C. Smith, "Multi-axial homogenized energy model for ferrolectric materials," 2006 ASME International Mechanical Engineering Congress and Exposition, Chicago, IL, IMECE2006-13733.

[17] W.S. Oates and R.C. Smith, "Nonlinear perturbation control for magnetic transducers," Proc 45th IEEE Conf. Dec. and Control, San Diego, CA, December 13-15, pp. 2441–2446, 2006.

[18] W.S. Oates and R.C. Smith, "Nonlinear optimal control techniques for vibration attenuation using magnetostrictive actuators," *Journal of Intelligent Material Systems and Structures*, to appear.

[19] W.S. Oates and R.C. Smith, "Optimal tracking using magnetostrictive transducers operating in the nonlinear and hysteretic regime," *Journal of Dynamic Systems, Measurement, and Control*, submitted.

[20] W.S. Oates and R.C. Smith, "Nonlinear control design for a piezoelectric-driven nanopositioning stage," *Journal of Dynamic Systems, Measurement, and Control*, submitted.

[21] S. Seelecke, S-J. Kim, B. Ball and R.C. Smith, "A rate-dependent two-dimensional free energy model for ferroelectric single crystals," *Continuum Mechanics and Thermodynamics*, 17(4), pp. 337-350, 2005.

[22] R.C. Smith, *Smart Material Systems: Model Development*, SIAM, Philadelphia, 2005.

[23] R.C. Smith and M.J. Dapino, "A homogenized energy model for the direct magnetomechanical effect," *IEEE Transactions on Magnetics*, 42(8), pp. 1944-1957, 2006.

[24] R.C. Smith, M.J. Dapino, T.R. Braun and A.P. Mortensen, "A homogenized energy framework for ferromagnetic hysteresis," *IEEE Transactions on Magnetics*, 42(7), pp. 1747-1769, 2006.

[25] R.C. Smith and A.G. Hatch, "Parameter estimation techniques for a class of nonlinear hysteresis models," *Inverse Problems*, 21, pp. 1363-1377, 2005.

[26] R.C. Smith, A.G. Hatch, T. De, M.V. Salapaka, R.C.H. del Rosario and J.K. Raye, "Model development for atomic force microscope stage mechanisms," *SIAM Journal on Applied Mathematics*, 66(6), pp. 1998-2026, 2006.

[27] R.C. Smith, A.G. Hatch, B. Mukherjee and S. Liu, "A homogenized energy model for hysteresis in ferroelectric materials: General density formulation," *Journal of Intelligent Material Systems and Structures*, 16(9), pp. 713-732, 2005.

[28] R.C. Smith and C.L. Hom, "A temperature-dependent constitutive model for relaxor ferroelectrics," *Journal of Intelligent Material Systems and Structures*, 16(5), pp. 433-448, 2005.

[29] R.C. Smith, S. Seelecke, M.J. Dapino and Z. Ounaies, "A unified framework for modeling hysteresis in ferroic materials," *Journal of the Mechanics and Physics of Solids*, 54(1), pp. 46-85, 2005.

[30] L.M. Weiland, E.K. Lada, R.C. Smith and D.J. Leo, "Application of rotational isomeric state theory to ionic polymer stiffness predictions," *Journal of Materials Research*, 20(9), pp. 2443–2455, 2005.